A Water-stable Tetranuclear Cd(II) Bicyclic Complex Used for the Picric Acid Detection①

WANG Ming WANG Xiao-Mei CHEN Ming-Yu
LIU Cheng DING Ge ZHOU Xin-Hui②

(*Key Laboratory for Organic Electronics and Information Displays & Jiangsu Key Laboratory for Biosensors, Institute of Advanced Materials* (*IAM*), *Jiangsu National Synergetic Innovation Center for Advanced Materials* (*SICAM*), *Nanjing University of Posts & Telecommunications, Nanjing* 210023, *China*)

ABSTRACT By solvothermal reaction of Cd(II) with organic ligand N,N′-bis(3,5-dicarboxylphenyl)-thiophene-2,5-dicarboxamide (H_4L), a water-stable complex $[Cd_4(H_2L)_4(H_2O)_{10}]\cdot 2CH_3OH\cdot 8H_2O\cdot 4DMF$ (**1**, $C_{102}H_{120}Cd_4N_{12}O_{64}S_4$) has been successfully synthetized (DMF = N,N-dimethylformamide). **1** crystallizes in the triclinic space group of $P\bar{1}$ with a = 11.815(7), b = 16.209(9), c = 16.742(9) Å, α = 82.224(13)°, β = 76.741(13)°, γ = 70.313(12)°, V = 2932(3) Å^3, M_r = 3115.93, Z = 1, F(000) = 1584, D_c = 1.765 Mg/cm^3, μ = 0.901 mm^{-1}, *GOOF* = 1.101, the final R = 0.0391 and wR = 0.1297 for 9007 observed reflections ($I > 2\sigma(I)$). **1** is a tetranuclear Cd(II) bicyclic complex with strong ligand-based blue emission and can stably exist in aqueous solutions over the pH range of 2~11. **1** exhibits high sensitivity, selectivity and anti-interference capability for picric acid (PA) detection in aqueous solution by luminescent quenching. The value of quenching constant (K_{sv}) is 3.2 × 10^4 M^{-1} within the PA concentration range of 0~40 μM and the detection limit is 6.89 × 10^{-7} M. Lastly, we went into depth on possible mechanism of the luminescent quenching.

Keywords: **sensors, complex, picric acid, fluorescence; DOI: 10.14102/j.cnki.0254-5861.2011-3182**

1 INTRODUCTION

As people pay more and more attention to health and safety issues, there is a growing demand for effective detection of nitroaromatic compounds. Among them, picric acid, a toxic pollutant and highly explosive molecule, is particularly noteworthy. It is widely used in the production of fireworks, dyes, pesticides and landmines[1, 2]. Therefore, it is necessary to develop a convenient and effective method to detect PA in aqueous solution.

As a new type of organic-inorganic hybrid materials, coordination complexes have broad prospects for development[3, 4]. It shows unique characteristics, including large specific surface area, well-defined structure, etc[5, 6]. Therefore, complexes can be extensively used in numerous fields, containing catalysis[7], gas separation[8], sensing[9, 10] and other functional materials[11]. Currently, luminescent complexes have been greatly researched as sensors to detect metal ions[12, 13], anions[14, 15], small molecules[16, 17], pH[18], and so on. As a connecting component, organic ligand plays a vital role in the performance of complex materials. In the past few decades, most studies have been focused on specific ligands, especially the carboxylate, pyrene and pyridine ligands[19-23]. While, the ligands containing thiophere ring have received little attention, which can exhibit excellent electron-transfer capabilities[2]. In addition, aromatic carboxylate ligands with π-conjugated system have strong coordination effects and can greatly affect luminescent properties[24, 25]. Importantly, π-electron-rich complexes could be excellent sensors to detect π-electron-deficient nitroaromatic compounds due to the photo induced electron-transfer mechanism[26-28]. At present, there are still challenges in designing and synthesizing coordination complexes with excellent stability[29]. Therefore, we tried to use the strategy of carboxylate ligands with sulfur rings to construct stable coordination complex materials.

Received 18 March 2021; accepted 8 June 2021 (**CCDC 2047887**)

① This research was supported by the National Natural Science Foundation of China (21973047) and Jiangsu Province Double Innovation Talent Program (090300014001)

② Corresponding author. E-mail: iamxhzhou@njupt.edu.cn

In this work, we report a new coordination complex $[Cd_4(H_2L)_4(H_2O)_{10}]\cdot 2CH_3OH\cdot 8H_2O\cdot 4DMF$ (**1**, $C_{102}H_{120}Cd_4N_{12}O_{64}S_4$), based on a carboxylate ligand N,N′-bis(3,5-dicarboxylphenyl)-thiophene-2,5-dicarboxamide (H_4L). **1** exhibits good chemical stability, which can keep structural integrity not only in water and air for at least three months but also in the aqueous solutions over the pH range of 2~11. It is particularly worth mentioning that **1** is an excellent luminescence probe for detecting PA with high sensitively and selectively. In addition, the possible luminescent quenching mechanisms towards PA have also been discussed in detail.

2 EXPERIMENTAL

2. 1 General

The ligand was synthesized according to the literature[30]. All other reagents were purchased commercially and used without any purification.

Elemental analyses (C, H, N) were carried out on a Perkin-Elmer 240C analyzer. FT-IR spectra were measured in the range of 400~4000 cm^{-1} with a PerkinElmer-Spectrum on KBr pellets. The thermogravimetric analyses (TGA) were preformed from room temperature to 800 ℃ under a nitrogen atmosphere on a NETZSCH STA2500 simultaneous DTA-TG apparatus instrument. Powder X-ray diffraction patterns (PXRD) data of all samples were collected in the 5~50 °range of 2θ with a scan step width of 0.02 ° on a Bruker D8 Advance A25 diffractometer (Cu$K\alpha$, λ = 1.5418 Å). The UV-Vis absorption spectra were recorded on a LAMBDA 35 spectrophotometer. Photoluminescence spectra were carried out using a RF-5301PC spectrofluorophotometer at room temperature.

2. 2 Synthesis

A mixture of $CdCl_2\cdot 2.5H_2O$ (138.4 mg, 0.6 mmol), N,N′-bis(3,5-dicarboxylphenyl)-thiophene-2,5-dicarboxamide(50 mg, 0.01 mmol), DMF (3 mL), H_2O (3 mL), CH_3OH (1 mL) and 4 drops of an aqueous HCl solution (0.2 M) was sealed into a 25 mL Teflon-lined stainless-steel container. The container was heated at 70 ℃ for 3 days. After the autoclave was cooled to room temperature, colorless needle crystals were obtained, washed with deionized water, and then dried in a vacuum oven. Elemental analysis calcd. for $C_{102}H_{120}Cd_4N_{12}O_{64}S_4$ (%): C, 39.32; N, 5.39; H, 3.88. Found: C, 39.35; N, 5.46; H, 3.80. IR (KBr pellet, cm^{-}): 3480 (b), 1656 (s), 1553 (vs), 1413 (m), 1330 (s), 1281 (m), 1247 (m), 907(vs), 768 (w), 699 (w), 594 (w), 435(w).

2. 3 Stability investigation

Aqueous solutions with different pH values, ranging from 2 to 12, were prepared. Then, samples were soaked in pH solution for 24 h, respectively. After centrifugation and drying, all the samples were performed PXRD measurement.

2. 4 Luminescence sensing

Unless otherwise specified, all luminescence measurements were executed in aqueous solution. A suspension of sample was prepared by adding 3 mg powder to 3 mL ultrapure water or ethanol under ultrasonic agitation for 30 minutes.

2. 5 X-ray crystallography

Single-crystal X-ray diffraction data were collected on a Bruker Smart Apex CCD diffractometer with graphite-monochromated Mo-$K\alpha$ radiation (λ = 0.71073 Å) at 100(2) K using an ω-θ scan mode in the range of $1.87\leqslant\theta\leqslant25.00$ °. Raw frame data were integrated with the SAINT program. The structure was solved by direct methods using SHELXS-2014[31] and refined by full-matrix least-squares on F^2 using SHELXL-2014[32]. An empirical absorption correction was applied with the program SADABS[33]. All non-hydrogen atoms were refined anisotropically. All hydrogen atoms were positioned geometrically and refined as riding atoms. The selected bond lengths and bond angles are showed in Table S1.

3 RESULTS AND DISCUSSION

3. 1 Structure of 1

X-ray single crystal diffraction analysis reveals that **1** crystallizes in triclinic space group $P\bar{1}$. The asymmetric unit of **1** includes two crystallographically unique Cd(II) ions, two partly deprotonated H_2L^{2-} ligands, five coordinated H_2O molecules, four uncoordinated H_2O molecules, one uncoordinated CH_3OH molecule and two uncoordinated DMF molecules (Fig. 1a). Each Cd(II) ion is coordinated by seven oxygen atoms, four of which are from two H_2L^{2-} ligands, and three from three H_2O molecules, forming the pentagonal bipyramidal coordination geometry. The four carboxyl groups of the two L^{4-} ligands chelate with two Cd(II) ions to form a Cd_2L_2 ring, and such two Cd_2L_2 rings are further connected by two water molecules double-bridging two Cd(II) ions to form a tetranuclear Cd(II) bicyclic complex, which are stacked into a 3D supramolecular structure (Fig. 1b). The porosity of **1** is 25.2%.

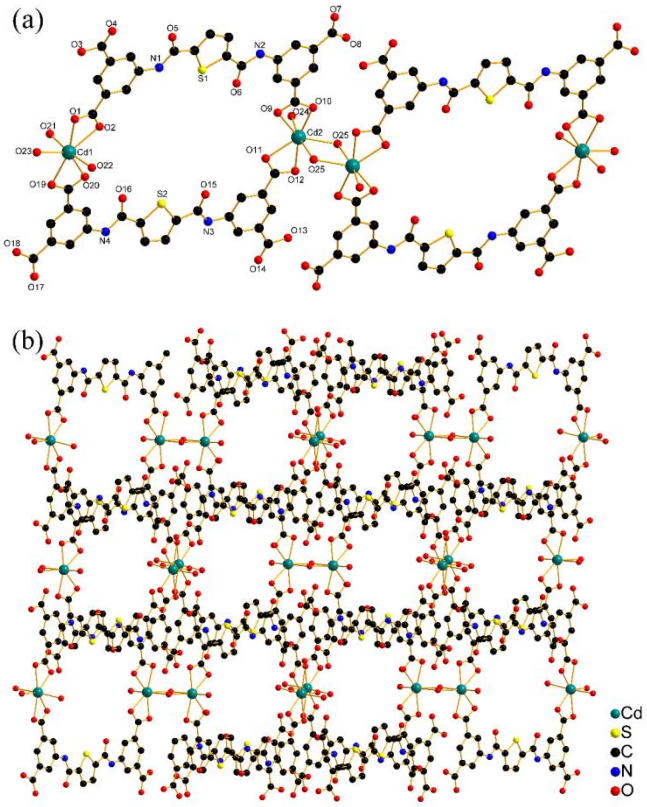

Fig. 1. (a) Two connected asymmetric units of 1 with thermal ellipsoids drawn at the 50% probability level; (b) 3D packing diagram of 1. All hydrogen atoms, H_2O, CH_3OH and DMF molecules are omitted for clarity

3. 2 TGA and PXRD of 1

Thermo-gravimetric analysis (TGA) of **1** was performed under a nitrogen atmosphere (Fig. S1). The first weight loss of 12.66% occurs from room temperature to 102 ℃, corresponding to the removal of two uncoordinated CH_3OH molecules, eight uncoordinated H_2O molecules and ten coordinated H_2O molecules (calcd. 12.46%). Then, the second weight loss of 9.40% in the temperature range of 102~330 ℃ is consistent with the departure of four uncoordinated DMF molecules (calcd. 9.38%). Further heating results in the decomposition of the organic ligands.

Powder X-ray diffraction of **1** was carried out in order to verity the phase purity and chemical stability. As shown in Fig. S2, the PXRD pattern of as-synthesized **1** keeps in good agreement with the simulated one, demonstrating high phase purity of the as-synthesized sample. Additionally, the PXRD patterns of the sample in different solvents, acidic and basic aqueous solutions (pH range of 2~12) for 24 h were obtained (Fig. S2 and S3), indicating that **1** possessed excellent chemical stability.

The IR spectra of free ligand and **1** are tested, and the results are presented in Fig. S4. Distinctly, an absorption band centered at 1705 cm^{-1} is observed in ligand, which is ascribed to the stretching vibration of C=O bond of the carboxyl groups. But it is absent in **1**, indicating the ligand was coordinated with Cd(II). Moreover, the broad peak at 3750~2500 cm^{-1} further confirmed the presence of H_2O molecules in **1**. The strong absorption at 1553 cm^{-1} is attributed to the C=N stretching vibration.

3. 3 Luminescence properties

The luminescence properties of H_4L and **1** are investigated in the solid state at room temperature. As shown in Fig. 2, the H_4L exhibits a luminescent emission peak at 450 nm upon excitation at 363 nm. **1** displays an emission peak at 463 nm when excited at 375 nm. By comparing the fluorescence spectra of **1** and H_4L, we can see that they keep a high degree of similarity, so the fluorescence emission of **1** mainly comes from the inherent properties of the ligand itself. In addition, a 13 nm red shift of **1** compared to the H_4L is observed, which may be attributed to the enhancement of ligand rigidity after coordination[6].

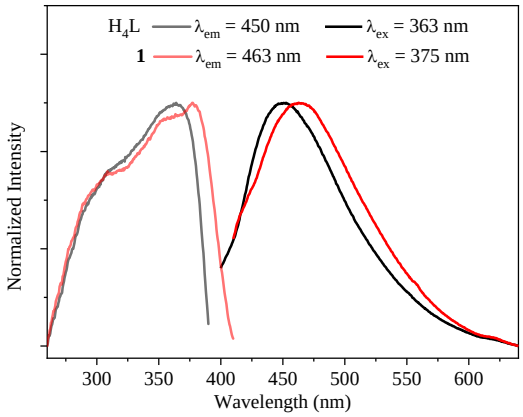

Fig. 2. Fluorescence spectra of 1 in solid state at room temperature

3. 4 Sensing of nitroaromatic compounds

The luminescence properties of **1** in different solvents are further measured. It is worth pointing out that the intensity of **1** in water is the strongest (Fig. S5). Additionally, **1** is stable after immersion in water for 3 months, as confirmed by the PXRD patterns (Fig. 3). So, unless otherwise specified, all luminescence measurements were executed in aqueous solution.

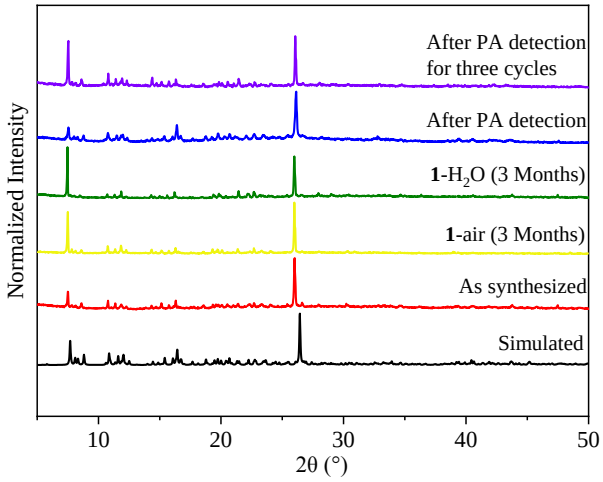

Fig. 3. X-ray powder diffraction patterns of sample 1 in water/air for 3 months

In order to explore the luminescence response of **1** towards various nitro explosive, 3.0 mg sample of **1** was ground and dispersed in 3.0 mL water or ethanol, then we kept them in ultrasonic treatment for 30 minutes. Considering the solubility, for the detections of 2,4-dinitrotoluene (2,4-DNT), 3,4-dinitrotoluene (3,4-DNT), 4-nitrotoluene (4-NT), 2-nitrotoluene (2-NT), 1,3-dinitrobenzene (1,3-DNB), 1,2-dinitrobenzene (1,2-DNB) and 2,3-dimethyl-2,3-dinitrobutane (DMNB), ethanol was used as the dispersion medium and solvent. While the detections for picric acid (PA), *p*-nitrophenol (4-NP), *m*-nitrophenol (3-NP) and *o*-nitrophenol (2-NP) were tested in both water and ethanol. The luminescence intensity at 463 nm of **1** after adding various nitroaromatic compounds (100 μM) in water or ethanol were displayed in Fig. 4. Obviously, the order of quenching percentage in aqueous solution is PA > 2-NP > 4-NP > 3-NP. When ethanol is used as the dispersion medium, PA still possesses the most remarkable quenching capacity towards **1**. Specifically, PA shows 87.8% quenching effect in water and 77% in ethanol. Additionally, competitive experiment was carried out by adding equal amount of other nitroaromatic compounds to **1**-ethanol suspension containing PA, respectively. It could be clearly observed that other nitroaromatic compounds did not interfere with the sensing ability of **1** for PA (Fig. S6). These results indicate that **1** possesses a good selective luminescence response towards PA.

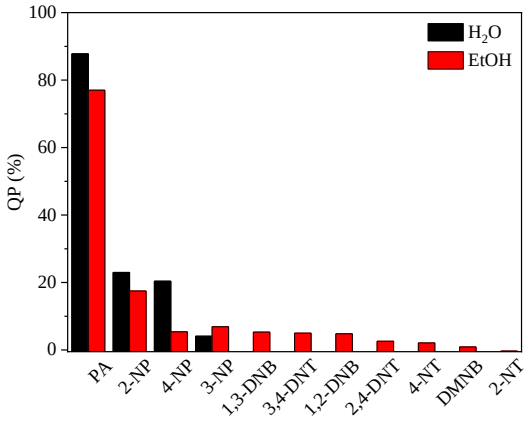

Fig. 4. Quenching efficiency of emission intensity of 1 with different nitro compounds in water/ethanol (50 μmol/L)

To further evaluate the sensitivity of **1** for sensing PA, the quantitative titration experiments were conducted. Besides, luminescence quenching titrations of 2-NP, 3-NP and 4-NP were also performed to compare with PA (Fig. S7). As shown in Fig. 5a, with increasing the PA concentration (0~250 μM), the luminescent intensity at 463 nm of **1** suspension decreased gradually. The emission of **1** was quenched completely when the concentration of PA was 150 μM. It is worth pointing out that the maximum emission at 463 nm shifts gradually to 483 nm upon the addition of PA. It can be seen that the I_0/I and the concentration of PA keep a good linear relationship (R^2 = 0.991) during the concentration range from 0 to 40 μM (Fig. 5b). According to the Stern-Volmer (SV) equation, the K_{sv} value is calculated to be 3.2×10^4 M^{-1}. The limit of detection was up to 6.89×10^{-7} M. In addition, the K_{sv} values are 3.82×10^3 M^{-1} for 2-NP, 8.11×10^2 M^{-1} for 3-NP and 2.85×10^3 M^{-1} for 4-NP, respectively.

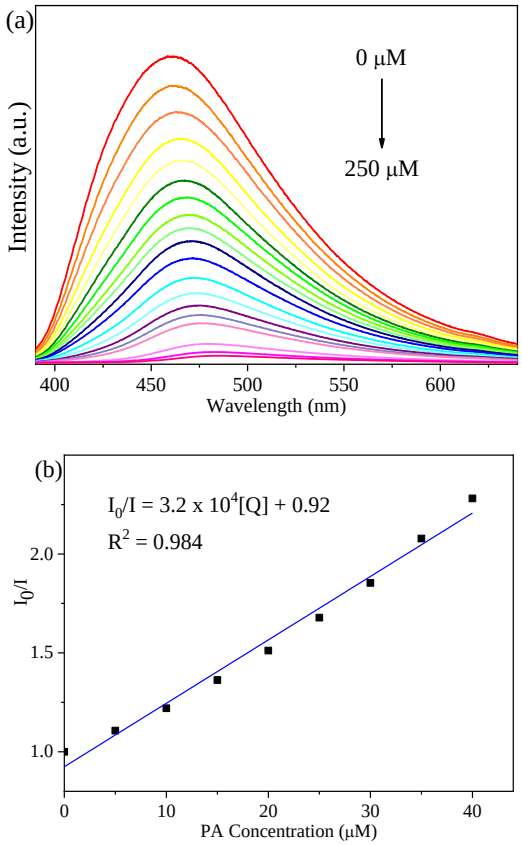

Fig. 5. (a) Emission spectra of 1 after adding different concentrations of PA; (b) Stern-Volmer curve for PA in the concentration range of 0~40 μmol/L

The regeneration of a sensor is also a vital factor toward its practical applications. The recycling experiment was carried out. After each round of testing, we collected **1** by centrifugation and washed it with water. As shown in Fig. 6, the luminescence intensity of **1** can almost be regained after washing. These results strongly advocate that **1** has good recyclability, which means it can be a promising sensor for the practical use.

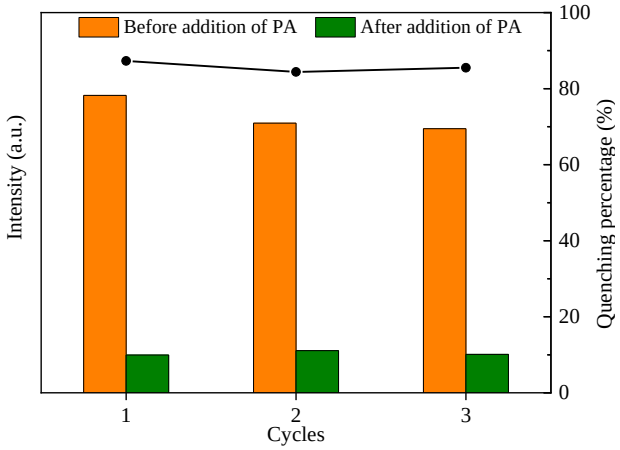

Fig. 6. Three cycles test of 1 suspension for detecting PA (30 μM)

3. 5 Sensing mechanism

We investigated the luminescence quenching mechanisms in order to better understand the reason behind quenching of **1** towards PA. We first attempted to verify whether the framework structure collapsed. As shown in Fig. 3, the PXRD pattern of sample after detection is consistent with the as-synthesized one. Therefore, **1** still keeps structural integrity during the sensing progress. There is no obvious change in IR spectra of **1** before and after the PA detecting test (Fig. S2), which can prove the above view from the other side. Secondly, the absorption spectra of nitroaromatic compounds were recorded in ethanol. We could know that the higher the spectral overlap between the absorbance spectrum of nitroaromatic compounds and excitation spectrum of **1**, the greater the probability of competitive absorption, so higher luminescence quenching percentage occurred. As shown in Fig. 7, the absorption band of PA from 300 to 450 nm shows the highest overlap with the excitation spectrum of **1**, indicating the reason of higher quenching percentage of PA. In addition, there also exists overlap between the emission spectrum of **1** and absorption spectrum of PA in ethanol. Thus, the resonance energy transfer (RET) is another possible reason for luminescence quenching. Moreover, a red shift in the maximum emission of **1** suspension after adding PA could be observed, indicating electrostatic interactions between PA and electron-rich **1**. Finally, according to previous literature, -OH group on PA and Lewis basic -N sites on **1** can form strong intermolecular interactions [34]. In a word, competitive absorption, RET and electrostatic interactions are mainly responsible for the luminescent quenching.

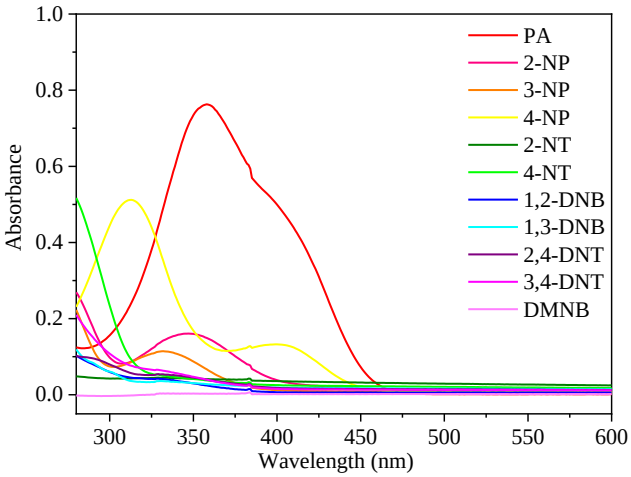

Fig. 7. UV-Vis adsorption spectra of various nitro compounds

4 CONCLUSION

In summary, a water-stable coordination complex **1** was successfully synthesized based on the solvothermal reaction of Cd(II) and organic ligand N,N′-bis(3,5-dicarboxylphenyl)-thiophene-2,5-dicarboxamide. **1** possesses excellent chemical stability in a wide pH range (2~11) and strong blue luminescence emission in water media. **1** could be employed as a luminescence probe to detect the PA multiple times with high sensitivity, selectivity and anti-interference. The possible quenching mechanisms could be attributed to the competitive absorption, RET and electrostatic interactions.

REFERENCE

(1) Xu, T.Y.; Li, J. M.; Han, Y. H.; Wang, A. R.; He, K. H.; Shi, Z. F. A new 3D four-fold interpenetrated dia-like luminescent Zn(II)-based metal-organic framework: the sensitive detection of Fe^{3+}, $Cr_2O_7^{2-}$, and CrO_4^{2-} in water, and nitrobenzene in ethanol. *New J. Chem.* **2020**, 44, 4011–4022.

(2) Zhuang, X. R.; Zhang, X.; Zhang, N. X.; Wang, Y.; Zhao, L. Y.; Yang, Q. F. Novel multifunctional Zn metal-organic framework fluorescent probe demonstrating unique sensitivity and selectivity for detection of PA and Fe^{3+} ions in water solution. *Cryst. Growth Des.* **2019**, 19, 5729–5736.

(3) Jiang, W.; Yang, J. Q.; Yan, G. S.; Zhou, S.; Liu, B.; Qiao, Y.; Zhou, T. Y.; Wang, J. J.; Che, G. B. A novel 3-fold interpenetrated *dia* metal-organic framework as a heterogeneous catalyst for CO_2 cycloaddition. *Inorg. Chem. Commun.* **2020**, 3, 113, 10770.

(4) Ren, S. S.; Jiang, W.; Wang, Q, W.; Li, Z. M.; Qiao, Y.; Che, G. B. Synthesis, structures and properties of six lanthanide complexes based on a 2-(2-carboxyphenyl)imidazo(4,5-*f*)-(1,10)phenanthroline ligand. *RSC Adv.* **2019**, 9, 3102–3112.

(5) Zhu, J. Y.; Xia, T. F.; Cui, Y. J.; Yang, Y.; Qian, G. D. A turn-on MOF-based luminescent sensor for highly selective detection of glutathione. *J. Solid State Chem.* **2019**, 270, 317–323.

(6) Fan, K.; Bao, S. S.; Nie, W. X.; Liao, C. H.; Zheng, L. M. Iridium(III)-based metal-organic frameworks as multiresponsive luminescent sensors for Fe^{3+}, $Cr_2O_7^{2-}$, and ATP^{2-} in aqueous media. *Inorg. Chem.* **2018**, 57, 1079–1089.

(7) Luz, I.; Parvathikar, S.; Carpenter, M.; Bellamy, T.; Amato, K. MOF-derived nanostructured catalysts for low-temperature ammonia synthesis. *J. Carpenter, M. Lail, Catal. Sci. Technol.* **2020**, 10, 105–112.

(8) Li, Y. Z.; Wang, G. D.; Yang, H. Y.; Hou, L.; Wang, Y. Y.; Zhu, Z. H. Novel cage-like MOF for gas separation, CO_2 conversion and selective adsorption of an organic dye. *Inorg. Chem. Front*. **2020**, 7, 746–755.

(9) Guo, H.; Wu, N.; Xue, R.; Liu, H.; Li, L.; Wang, M. Y.; Yao, W. Q.; Li, Q.; Yang, W. Multifunctional Ln-MOF luminescent probe displaying superior capabilities for highly selective sensing of Fe^{3+} and Al^{3+} ions and nitrotoluene. *Colloid Surface A* **2020**, 585, 124094.

(10) Moradi, E.; Rahimi, R.; Farahani, Y. D.; Safarifard, V. Porphyrinic zirconium-based MOF with exposed pyrrole Lewis base site as a luminescent sensor for highly selective sensing of Cd^{2+} and Br^- ions and THF small molecule. *J. Solid State Chem.* **2020**, 282, 121103.

(11) Igoa, F.; Peinado, G.; Suescun, L.; Kremer, C.; Torres, J. Design of a white-light emitting material based on a mixed-lanthanide metal organic framework. *J. Solid State Chem.* **2019**, 279, 120925.

(12) Zhan, Z. Y.; Liang, X. Y.; Zhang, X. L.; Jia, Y. J.; Hu, M. A water-stable europium-MOF as a multifunctional luminescent sensor for some trivalent metal ions (Fe^{3+}, Cr^{3+}, Al^{3+}), PO_4^{3-} ions, and nitroaromatic explosives. *Dalton Trans.* **2019**, 48, 1786–1794.

(13) Xiao, J. N.; Liu, J. J.; Gao, X. C.; Ji, G. F.; Wang, D. B.; Liu, Z. L. A multi-chemosensor based on Zn-MOF: ratio-dependent color transition detection of Hg(II) and highly sensitive sensor of Cr (VI). *Sensor Actuat. B-Chem.* **2018**, 269, 164–172.

(14) Xu, H.; Xiao, Y. Q.; Rao, X. T.; Dou, Z. S.; Li, W. F.; Cui, Y. J.; Wang, Z. Y.; Qian, G. D. A metal-organic framework for selectively sensing of PO_4^{3-} anion in aqueous solution. *J Alloys Compd.* **2011**, 509, 2552–2554.

(15) Qin, Y. R.; Ge, Y.; Zhang, S. S.; Sun, H.; Jing, Y.; Li, Y. H.; Liu, W. A series of Ln_4^{III} clusters: Dy_4 single molecule magnet and Tb_4 multi-responsive luminescent sensor for Fe^{3+}, CrO_4^{2-}/$Cr_2O_7^{2-}$ and 4-nitroaniline. *RSC Adv.* **2018**, 8, 12641–12652.

(16) Yang, Y.; Chen, L.; Jiang, F. L; Wu, M. Y.; Pang, J. D.; Wan, X. Y.; Hong, M. C. A water-stable 3D Eu-MOF based on a metallacyclodimeric secondary building unit for sensitive fluorescent detection of acetone molecules. *CrystEngComm.* **2019**, 21, 321–328.

(17) Cui, Y.; Chen, F.; Yin, X. B. A ratiometric fluorescence platform based on boric-acid-functional Eu-MOF for sensitive detection of H_2O_2 and glucose. *Biosens Bioelection* **2019**, 135, 208–215.

(18) Yu, L.; Zheng, Q. T.; Wu, D.; Xiao, Y. X. Bimetal-organic framework nanocomposite based point-of-care visual ratiometric fluorescence pH microsensor for strong acidity. *Sensor Actuat. B-Chem.* **2019**, 294, 199–205.

(19) Liu, W.; Wang, Y. L.; Song, L. P.; Silver, M. A.; Xie, J.; Zhang, L. M.; Chen, L. H.; Diwu, J.; Chai, Z. F.; Wang, S. Efficient and selective sensing of Cu^{2+} and UO_2^{2+} by a europium metal-organic framework. *Talanta* **2019**, 196, 515–522.

(20) Zhou, X. H.; Chen, Q. Q.; Liu, B. L.; Li, L.; Yang, T.; Huang, W. Syntheses, structures and magnetic properties of nine coordination polymers based on terphenyl-tetracarboxylic acid ligands. *Dalton Trans.* **2017**, 46, 430–444.

(21) Fu, H. R.; Wu, X. X.; Ma, L. F.; Wang, F.; Zhang, J. Dual-emission SG7@MOF sensor via SC–SC transformation: enhancing the formation of excimer emission and the range and sensitivity of detection. *ACS Appl. Mater. Interfaces* **2018**, 10, 18012–18020.

(22) Luo, J.; Liu, B. S.; Zhang, X. R.; Liu, R. T. A Eu^{3+} post-functionalized metal-organic framework as fluorescent probe for highly selective sensing of Cu^{2+} in aqueous media. *J. Mol. Struct.* **2019**, 1177, 444–448.

(23) Wu, K. Y.; Qin, L.; Fan, C.; Cai, S. L.; Zhang, T. T.; Chen, W. H.; Tang, X. Y.; Chen, J. X. Sequential and recyclable sensing of Fe^{3+} and ascorbic acid in water with a terbium(III)-based metal-organic framework. *Dalton Trans.* **2019**, 48, 8911–8919.

(24) Feng, X.; Guo, N.; Li, R. F.; Chen, H. P.; Ma, L. F.; Li, Z. J.; Wang, L. Y. A facile route for tuning emission and magnetic properties by controlling lanthanide ions in coordination polymers incorporating mixed aromatic carboxylate ligands. *J. Solid State Chem.* **2018**, 268, 22–29.

(25) Li, R.; Qu, X. L.; Zhang, Y. H.; Han, H. L.; Li, X. Lanthanide-organic frameworks constructed from naphthalenedisulfonates: structure, luminescence and luminescence sensing properties. *CrystEngComm.* **2016**, 18, 5890–5900.

(26) Cao, A. P.; Zhu, W.; Shang, J.; Klootwijk, J. H.; Sudhölter, E. J. R.; Huskens, J.; de Smet, L. C. P. M. Metal-organic polyhedra-coated Si nanowires for the sensitive detection of trace explosives. *Nano Lett.* **2017**, 17, 1–7.

(27) Wu, X. X.; Fu, H. R.; Han, M. L.; Zhou, Z.; Ma, L. F. Tetraphenylethylene immobilized metal-organic frameworks: highly sensitive fluorescent sensor for the detection of $Cr_2O_7^{2-}$ and nitroaromatic explosives. *Cryst. Growth Des.* **2017**, 17, 6041–6084.

(28) Hu, Y. L.; Ding, M. L.; Liu, X. Q.; Sun, L. B.; Jiang, H. L. Rational synthesis of an exceptionally stable Zn(II) metal-organic framework for the highly selective and sensitive detection of picric acid. *Chem. Commun.* **2016**, 52, 5734–5737.

(29) Liang, Y. T.; Yang, G. P.; Liu, B.; Yan, Y. T.; Xia, Z. P.; Wang, Y. Y. Four super water-stable lanthanide-organic frameworks with active uncoordinated carboxylic and pyridyl groups for selective luminescence sensing of Fe^{3+}. *Dalton Trans.* **2015**, 44, 13325–13330.

(30) Wang, G. Y.; Song, C.; Kong, D. M.; Ruan, W. J.; Chang, Z.; Li, Y. Two luminescent metal-organic frameworks for the sensing of nitroaromatic explosives and DNA strands. *J. Mater. Chem. A* **2014**, 2, 2213–2220.

(31) Sheldrick, G. M. *SHELXS-2014*, *Program for Crystal Structure Solution*. University of Gottingen, Germany **2014**.

(32) Sheldrick, G. M. *SHELXL-2014*, *Program for the Refinement of Crystal Structure*. University of Gottingen, Germany **2014**.

(33) Sheldrick, G. M. *SADABS*, *Program for Empirical Absorption Correction of Area Detector Data*. University of Gottingen, Gottingen Germany **1997**.

(34) Chen, D. M.; Zhang, N. N.; Liu, C. S.; Du, M. Dual-emitting dye@MOF composite as a self-calibrating sensor for 2,4,6-trinitrophenol. *ACS Appl. Mater. Interfaces* **2017**, 9, 24671–24677.